DOI: 10.1002/ejoc.200600105

A DFT Study of the Molecular Mechanisms of the Nucleophilic Addition of Ester-Derived Lithium Enolates and Silyl Ketene Acetals to Nitrones: Effects of the Lewis Acid Catalyst

Luis R. Domingo,*[a] Manuel Arnó,[a] Pedro Merino,*[b] and Tomás Tejero[b]

Keywords: Acetals / Density functional calculations / Enolates / Nucleophilic addition / Reaction mechanisms

The molecular mechanisms for the nucleophilic addition of lithium enolates and silyl ketene acetals to nitrones in the absence and in the presence of a Lewis acid (LA) catalyst to give isoxazolidin-5-ones or hydroxylamines have been investigated by DFT methods at the B3LYP/6-31G* level. The addition of lithium enolates to nitrones gives the corresponding hydroxylamines, while the addition of silyl ketene acetals affords isoxazolidin-5-ones through a concerted 1,3-dipolar cycloaddition. The addition of the silyl ketene acetals to LA-coordinated nitrones yields isoxazolidin-5-ones by a polar concerted cycloaddition or a stepwise nucleophilic attack via zwitterionic intermediates. A silyl migration on the [3+2] cycloadduct yields the corresponding *O*-silylhydroxylamine. An analysis of the global electrophilicity of the reagents accounts for the strong electrophile activation of the LA-coordinated nitrone, and the analysis of the local indices leads to an explanation for the experimentally observed regioselectivity.

Introduction

The nucleophilic addition of enolates to imines and related compounds (the so-called Mannich-type reactions) is an important tool in organic synthesis,[1] and a variety of electrophiles have been used for the synthesis of the resulting nitrogen-containing compounds. In addition to imines,[2] other C=N functionalities, including hydrazones,[3] nitrones,[4] and iminium salts,[5] have also been utilized.

Of particular importance are reactions with ester-derived nucleophiles, such as lithium/sodium and silyl ketene acetals, which lead to β-amino acids (Scheme 1).[6] In this respect, nitrones have emerged as key synthons in their synthesis, and several diastereo-[7] and enantioselective[8] approaches, based on the process illustrated in Scheme 1, have been reported.

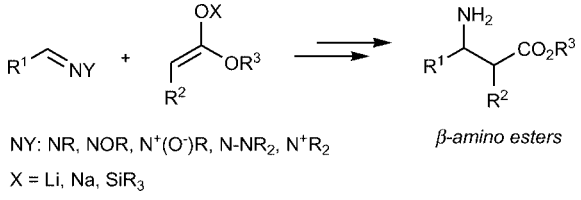

Scheme 1.

The mechanism of the addition of ketene acetals to nitrones has been controversial, and several options have been discussed to date by several authors. Thus, the reaction could take place through a stepwise mechanism involving prior coordination of the nitrone oxygen atom to the lithium atom (Scheme 2, path A). This mechanism has been proposed by us[7g] for the addition of lithium ketene acetals, which takes place smoothly at low temperature. The same approach had been postulated by Tomoda et al.[9] and Murahashi et al.[7e] for silyl ketene acetals. The latter also invoked path A for both boron and titanium enolates.[10]

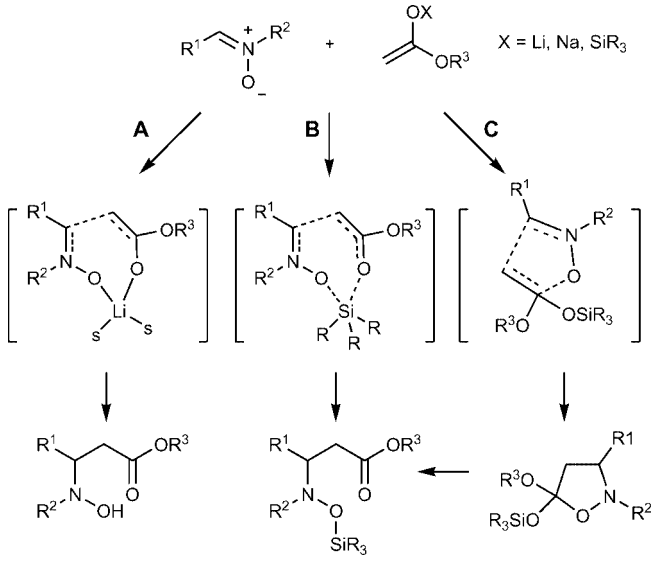

Scheme 2.

[a] Instituto de Ciencia Molecular, Departamento de Química Orgánica, Universidad de Valencia,
Dr. Moliner 50, 46100 Burjassot, Valencia, Spain
[b] Departamento de Quimica Organica, Facultad de Ciencias, ICMA, Universidad de Zaragoza,
50009 Zaragoza, Spain

Greene et al.[7a] have suggested a pentacoordinate silicon atom as a plausible transition structure (TS; Scheme 2, path B). This possibility, based on semiempirical calculations, was subsequently ruled out by us,[11] also using a semiempirical level of theory. The authors who initially proposed this approach have recently confirmed[12] that the mechanism illustrated in path B cannot explain several experimental findings, such as the formation of an orthoester.[13,14] In the particular case of the reaction with silyl ketene acetals, the process can also be considered to proceed as a classical concerted 1,3-dipolar cycloaddition (13DC; path C, Scheme 2). The migration of a further silyl group could explain the formation of open-chain products. This mechanism, recently confirmed by Greene et al.[12] and already discussed in a previous study,[11] could explain both the formation of orthoesters and silylated hydroxylamines. However, in the case of silicon derivatives the presence of a Lewis acid (LA) is needed for activation (no reaction is observed in the absence of an LA); therefore any study of this reaction should consider the presence of such an activator in order to be realistic.

The cycloaddition vs. nucleophilic process dichotomy is a central proposition in the reaction mechanism. A parallel assessment of both processes could be valuable depending on the atom (lithium vs. silicon) and the presence/absence of an LA. In order to gain insight about TSs on the basis of the reactivity, we report here a comparison between lithium and silyl ketene acetals; for the latter, the addition of an LA as an activator has also been studied. In particular, in the present study, the molecular mechanism for the nucleophilic addition of ester-derived lithium enolates and silyl ketene acetals to nitrones to give [3+2] cycloadducts, isoxazolidin-5-ones, or hydroxylamines has been investigated by DFT methods. For this purpose, the reaction of lithium 1-methoxyethenolate (**2**) with nitrone **1** (see Scheme 4), and the reactions of (1-methoxyvinyloxy)trimethylsilane (**5**) with nitrone **1**, in the absence and in the presence of BH_3·LA (see Schemes 5 and 6) have been investigated.

The article is structured as follows. The results are presented and discussed on the basis of the generated trends in terms of global and local electrophilicity indexes, and the analysis of stationary points on the potential energy surface (PES). This analysis allows us to rationalize and explain the experimental observations. Next, in the concluding section, the net outcome of the work is summarized. Finally, the selected computational techniques and methodologies are listed in the last section together with a brief theoretical background of the global and local electrophilicity indexes.

Results and Discussions

DFT Analysis Based on the Reactivity Indexes

Recent studies devoted to Diels–Alder[15] and 13DC[16] reactions have shown that the global and local indexes defined in the context of DFT[17] are a powerful tool to understand the behavior of polar cycloadditions. The static global properties, namely electronic chemical potential, μ, chemical hardness, η, and global electrophilicity, ω, of a series of nitrones and enolates are presented in Table 1.

Table 1. Electronic chemical potential (μ, in au), chemical hardness (η, in au), and global electrophilicity (ω, in eV) of nitrones **1** and **8** and enolates **2** and **5**.

	μ	η	ω
8	–0.1489	0.1656	1.82
11	–0.1260	0.2038	1.06
1	–0.1084	0.1993	0.80
12	–0.0893	0.2564	0.42
2	–0.0571	0.1550	0.29
5	–0.0729	0.2568	0.28

The electronic chemical potential of the lithium enolate **2** and the silyl ketene acetal **5** (μ = –0.0571 and –0.0729 au, respectively) are less than those for the nitrone **1** and the BH_3-coordinated nitrone **8** (μ = –0.1084 and –0.1489 au, respectively), thus indicating that along a polar interaction a net charge transfer (CT) will take place from these enolates towards the nitrones, in clear agreement with the CT analysis performed at the corresponding TSs (see later).

The electrophilicity of the simplest nitrone ($H_2C{=}N^+H{-}O^-$, **11**) is 1.06 eV, a value that falls in the range of moderate electrophiles within the ω scale.[16] Appropriate substitution on the nitrone can modify the electrophilicity such that it can participate in both normal- and inverse-electron-demand (IED) 13DC reactions.[16] The inclusion of two electron-releasing methyl groups on the simplest nitrone decreases the electrophilicity of **1** to 0.80 eV, at which point it is classified as a marginal electrophile. However, coordination of BH_3 to the nitrone oxygen atom increases the electrophilicity of **8** to 1.82 eV, where it is classified as a strong electrophile.[16] Therefore, it is expected that the LA-coordinated nitrones **8** will act as good electrophiles in polar processes. On the other hand, the lithium enolate **2** and silyl ketene acetal **5** have electrophilicity values of 0.29 and 0.28 eV, respectively, and are classified as marginal electrophiles (good nucleophiles). Note that the electrophilicity of these enolates is lower than that for methyl vinyl ether (MVE, **12**; 0.42 eV), which is used as a good nucleophile in polar cycloadditions.[18] A good correlation has been found for polar cycloaddition reactions between the difference of electrophilicity of the reagent pair, $\Delta\omega$, and the CT at the corresponding TS.[15,16] Consequently, $\Delta\omega$ has been used as a measure of the polar character of the cycloaddition. The $\Delta\omega$ for the reaction between nitrone **1** and silyl ketene acetal **5** has a low value (0.52 eV), thus indicating that the corresponding cycloaddition will have a low polar character. On the other hand, the LA-catalyzed cycloaddition of **5** and **8** has a $\Delta\omega$ value of 1.54 eV. The increase of $\Delta\omega$ for the catalyzed reaction relative to the uncatalyzed one suggests a more polar process with lower activation energy.

Analysis of the local electrophilicity[19] at the nitrone **1** and the LA-coordinated nitrone **8**, together with analysis of the nucleophilic Fukui functions[20] at the enolates **2** and **5**, allows us to characterize the more favorable two-center interaction along a polar process, and, as a consequence,

the more favorable regioisomeric reactive channel.[21] The values of the local indexes are summarized in Scheme 3. The nitrone **1** has a larger electrophilic activation at C3 (0.34 eV) than at O1 (0.14 eV; see Scheme 3). Coordination of LA·BH_3 to the nitrone O1 atom increases the electrophilicity of C3 to 0.96 eV, while this value at O1 drops slightly to 0.11 eV. The ω_k value at the C3 atom of LA-coordinated nitrone **8** is about three times the value of ω_k at the C1 atom of nitrone **1**. Therefore, C3 corresponds to the more favorable center of **8** for a nucleophilic attack.

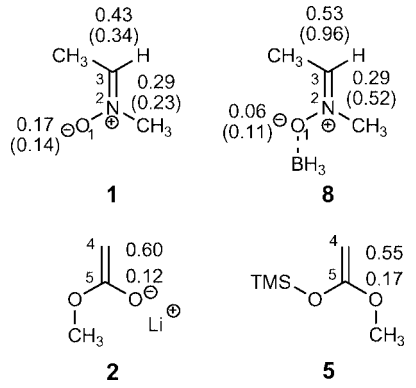

Scheme 3. Fukui functions for a nucleophilic attack and local electrophilicity (ω_k in eV, in parentheses) for **1** and **8**, and Fukui functions for electrophilic attack for **2** and **5**.

For the enolates **2** and **5**, analysis of the Fukui functions for an electrophilic attack indicates that C4 corresponds to the more nucleophilic site of these molecules. In consequence, along a polar reaction the more favorable reactive channel will correspond to that associated with a two-center interaction between the C3 atom of the nitrones and the C4 atom of the enolates.

Recently, the LA-catalyzed IED 13DC reaction of nitrone **1** with MVE to give exclusively the 5-substituted isoxazolidine has been studied experimentally by Jorgensen et al.[22] and theoretically by Domingo.[18] This 13DC reaction is completely regioselective. The TSs associated with the formation of isoxazolidines were about 13 kcal mol^{-1} lower in energy than those associated with the formation of the corresponding regioisomeric [3+2] cycloadducts. Analysis of the TSs associated with the formation of the isoxazolidines indicated that they are associated with the nucleophilic attack of the less substituted carbon atom of MVE to the nitrone carbon atom. These results are in complete agreement with the analysis of the regioselectivity based on the local indexes.

Analysis on the Basis of the Exploration of the PES

Study of the Reaction of Nitrone 1 with Lithium 1-Methoxyethenolate (2)

An exhaustive exploration of the PES for the addition of enolate **2** to nitrone **1** allows the discovery of one TS, **TS1**, associated with the attack of the most nucleophilic center of enolate **2** − the unsubstituted C4 atom − to the most electrophilic center of nitrone **1** − the C3 atom (see Scheme 4). The IRC from **TS1** to reactants gives a molecular complex, **MC1**, in which the lithium atom is coordinated to both the nitrone O1 and enolate O6 atoms. Along this reaction channel, the lithium atom is also coordinated to two ether molecules to complete the fourfold coordination sphere.[23] Although a TS associated with an *anti* approach of the C4–C5 double bond in **2** relative to the N2–C3 double bond in **1** was also found, the corresponding adduct is not stable; in addition, the corresponding activation energy associated with this *anti* approach is 3.5 kcal mol^{-1} higher in energy than **TS1**. The total and relative energies are summarized in Table 2, while the geometries of **TS1** and adduct **3** are given in Figure 1.

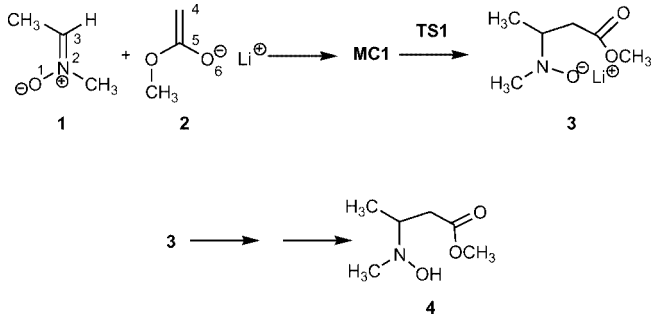

Scheme 4.

Table 2. Total (E, in au) and relative (ΔE, in kcal mol^{-1})[a] energies in vacuo and in dichloromethane of the stationary points involved in the addition of enolates **2** and **5** to nitrones **1** and **8**.

	E	ΔE	E_{sol}	ΔE_{sol}
Scheme 4				
MC1	–833.897015		–833.905843	
TS1	–833.895392	1.0	–833.901221	2.9
3	–833.918366	–13.4	–833.924540	–11.7
Scheme 5				
1	–248.435874		–248.440856	
5	–677.052151		–677.054178	
TS2	–925.462593	16.0	–925.465824	18.3
6	–925.541061	–33.3	–925.543963	–30.7
TS3	–925.450323	23.7	–925.455943	24.5
IN1	–925.454465	21.1	–925.459852	22.1
TS4	–925.496390	–5.2	–925.499413	–2.7
7	–925.550617	–39.3	–925.553889	–36.9
Scheme 6				
8	–275.0877094		–275.1016866	
5	–677.0521507		–677.054178	
TS5	–952.1290956	6.8	–952.1443083	7.3
9	–952.1686761	–18.1	–952.1758253	–12.5
TS6	–952.1267712	8.2	–952.1459892	6.2
IN2	–952.1337369	3.8	–952.1559062	0.0
Tsrot1	–952.1328886	4.4	–952.1537503	1.3
TS7	–952.1189681	13.1	–952.1472729	5.4
IN3	–952.1191914	13.0	–952.1499372	3.7
TSrot2	–952.1159508	15.0	–952.1460024	6.2
TS8	–952.1435632	–2.3	–952.1522177	2.3
10	–952.1898387	–31.4	–952.1953974	–24.8

[a] Relative to **MC1**, **1** + **5**, or **8** + **5**.

The activation energy associated with **TS1** from **MC1** is 2.9 (1.0) kcal mol^{-1}. Relative energies correspond to the PCM calculations (the corresponding gas-phase relative en-

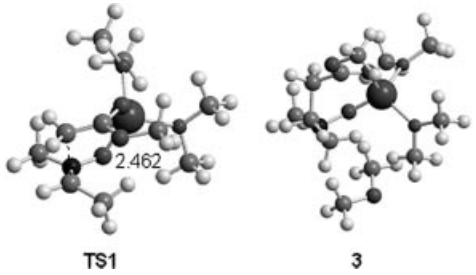

Figure 1. Geometries of the transition structures involved in the addition of lithium enolate **2** to nitrone **1** (**TS1**) and adduct **3**. The distances are given in Å. At **TS1** and **3** the lithium atom is coordinated to two ether molecules.

ergies are given in parentheses). Coordination of the lithium atom to the nitrone O1 and the enolate O6 atoms favors the nucleophilic attack of the enolate **2** to the nitrone **1** along the *gauche* reactive channel by an increase of the electrophilicity of the nitrone; consequently, the lithium atom acts as an LA catalyst, which favors the nucleophilic addition. Note that although enolate **2** is a good nucleophile, nitrone **1** is a poor electrophile. Formation of adduct **3** is exothermic by –11.7 (–13.4) kcal mol^{-1}. Further hydrolysis of adduct **3** affords the final hydroxylamine **4**.

The geometries of **TS1** and adduct **3** are given in Figure 1. The length of the forming C3–C4 bond at the *gauche* **TS1** is 2.462 Å. At this TS, the lithium atom is coordinated to the nitrone O1 and the enolate O6 atoms; the distance of the lithium atom to these oxygen atoms is 1.906 and 1.896 Å, respectively. The N2–C3–C4–C5 dihedral angle at the *gauche* **TS1** is –83.1°. At the adduct **3**, the C3–C4 bond length (1.588 Å) indicates that this bond is already formed, while the C5–O6 bond length (1.299 Å) corresponds to a C–O double bond. The distance of the lithium atom to the nitrone O1 and enolate O6 atoms is 1.788 and 1.964 Å, respectively. Along the reaction path, the lithium atom is transferred from the enolate O6 atom to the nitrone O1 atom.

The extent of bond formation along a reaction pathway is provided by the concept of bond order (BO).[24] Along the *gauche* reactive channel the BO values for the forming C3–C4 bond are 0.23 at **TS1** and 0.93 at the adduct **3**.

Natural population analysis (NPA) allows us to evaluate the CT along the nucleophilic attack of lithium enolate **2** to nitrone **1**. The natural charges of the TSs have been shared between the donor enolate and the acceptor nitrone frameworks, and the lithium atom. The natural charges for these fragments at **TS1** are –0.20 e for the **1** framework, –0.69 e for the **2** framework, and 0.89 e for the lithium atom. For adduct **3**, the natural charges for these fragments are –0.75 e for the **1** framework, –0.11 e for the **2** framework, and 0.85 e for the lithium atom. These data show that along the nucleophilic attack a large amount of charge is transferred from the enolate to the nitrone. Note that along the reaction channel, the CT is accompanied by the transfer of the lithium atom from the enolate O6 atom to the nitrone O1 one.

Study of the Reaction of Nitrone 1 with (1-Methoxyvinyloxy)trimethylsilane (5)

Two reactive channels have been characterized for the reaction between nitrone **1** and silyl ketene acetal **5**. They are related to the two *gauche* approaches, named as *1 gauche* and *2 gauche*, of the C4–C5 double bond of the silyl ketene acetal **5** to the N2–C3 one of nitrone **1** (see Scheme 5). All attempts to locate the TS associated with an *anti* approach were unsuccessful. A TS associated with the conversion of the [3+2] cycloadduct **6** into *O*-(trimethylsilyl)hydroxylamine (**7**) was also found. Therefore, three TSs (**TS2**, **TS3**, and **TS4**) and the reaction products **6** and **7** were located and characterized. Their total and relative energies are summarized in Table 2, and the geometries of the TSs are given in Figure 2.

TS2 is associated with the concerted 13DC reaction between nitrone **1** and silyl ketene acetal **5** to give the [3+2] cycloadduct **6**, an isoxazolidin-5-one, while **TS3** is associated with the nucleophilic attack of **5** to **1** to yield a zwitterionic intermediate, **IN1**, which, after a C3–C4 bond rotation, could afford the [3+2] cycloadduct **6** (see Scheme 5). Finally, O1–C5 bond breaking with concomitant migration of the TMS group from the O6 atom to the nitrone O1 atom at the cycloadduct **6** via **TS4** gives **7**. The activation energies associated with **TS2** and **TS3** are 18.3 (16.0) and 24.5 (23.7) kcal mol^{-1}, respectively. Formation of the [3+2] cycloadduct **6** is exothermic by –30.7 (–33.3) kcal mol^{-1}. The TS associated with the nucleophilic attack, **TS3**, is 6.2 kcal mol^{-1} higher in energy than that associated with the concerted [3+2] cycloaddition, **TS2**, and the zwitterionic in-

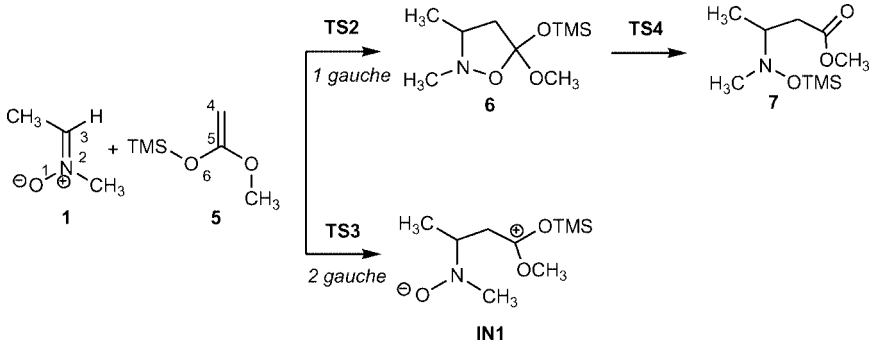

Scheme 5.

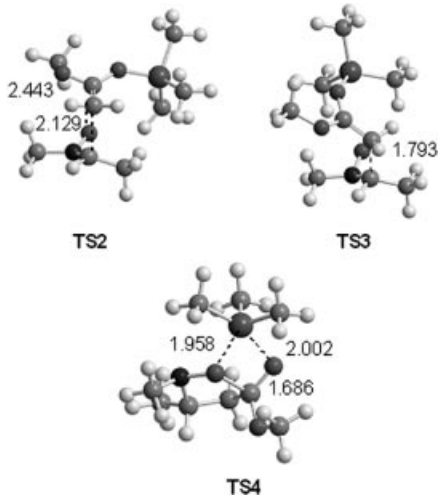

Figure 2. Geometries of the transition structures involved in the addition of silyloxy enolate **5** to the nitrone **1** (**TS2** and **TS3**) and the transition structures involved in the silyl migration (**TS4**). The distances are given in Å.

termediate **IN1** is located 22.1 (21.1) kcal mol^{-1} above the reagents. Therefore, formation of the intermediate **IN1** is kinetically and thermodynamically unfavorable and the nucleophilic attack is not competitive.

The activation energy for the attack of silyl ketene acetal **5** to nitrone **1** is 15.4 kcal mol^{-1} higher than that associated with the attack of enolate **2** to **1**. Two factors are responsible for this behavior: i) enolate **2** is more nucleophilic than the silyl ketene acetal **5**, and ii) coordination of the lithium atom of enolate **2** to the nitrone O1 atom of **1** catalyzes the nucleophilic addition very efficiently. Note that nitrone **1** has been classified as a poor electrophile.[16]

Finally, the activation energy associated with the conversion of the [3+2] cycloadduct **6** into **7** via **TS4** is 28.0 (28.1) kcal mol^{-1}. Hydroxylamine **7** is located 6.2 (6.0) kcal mol^{-1} below the cycloadduct **6**. Consequently, while cycloadduct **6** can be obtained under kinetic control, the barrier for the cycloaddition is 9.7 kcal mol^{-1} lower in energy than that associated with the conversion of **6** into **7**, which is therefore obtained by thermodynamic control.

The geometries of **TS2**, **TS3**, and **TS4** are given in Figure 2. The length of the forming C3–C4 and O1–C5 bonds at the most favorable *1 gauche* **TS2** are 2.129 and 2.443 Å, respectively. The extent of the asynchronicity of the bond formation at this concerted TS can be measured by means of the difference between the lengths of the two σ-bonds that are being formed in the reaction, i.e., $\Delta r = d$(O1–C5) – d(C3–C4). This value at **TS2** (Δr = 0.31) indicates that this TS corresponds to an asynchronous concerted bond-formation process where the formation of the C3–C4 bond is more advanced than the formation of the O1–C5 one. The length of the forming C3–C4 bond at the less favorable *2 gauche* **TS3** is 1.792 Å, while the distance between the O1 and C5 atoms is 3.345 Å. The shorter C3–C4 distance at **TS3** is in agreement with the large endothermic character of the formation of **IN1**. At the intermediate **IN1** the C3–C4 bond length (1.612 Å) indicates that the new σ-bond has already formed. The N2–C3–C4–C5 dihedral angles at the TSs are –22.5° at *1 gauche* **TS2** and 41.0° at *2 gauche* **TS3**. At the TS associated with the transformation of the [3+2] cycloadduct **6** into **7** (**TS4**) the distances between the O1 and C5, O6 and Si, and O1 and Si atoms are 1.686, 2.002, and 1.958 Å, respectively.

The BO values of the forming C3–C4 and O1–C5 bonds at the *1 gauche* **TS2** are 0.41 and 0.20, respectively. For this asynchronous concerted TS, the C3–C4 bond formation is more advanced than the O1–C5 one. Note that at this concerted process the asynchronicity of the bond formation is controlled by the more electrophilic site of the nitrone.[21] At the *2 gauche* **TS3** the C3–C4 BO value (0.67) indicates that the bond formation is very advanced. Finally, the BO values between the O1 and C5, O6 and Si, and O1 and Si atoms at **TS4** are 0.52, 0.30, and 0.32, respectively. These BO values indicate that both the breaking of the O1–C5 bond and the migration of the trimethylsilyl (TMS) group are coupled.

To evaluate the CT along the two *gauche* reactive channels associated with the attack of **5** to **1**, the natural charges at the TSs were shared between the donor silyl ketene acetal **5** and the acceptor nitrone **1**. The CT from **5** to **1** at the TSs is 0.13 e at **TS2** and 0.31 e at **TS3**. These values indicate that these species have some zwitterionic character. The more advanced *2 gauche* **TS2** presents a large CT. The low CT found for the concerted process is in agreement with the low $\Delta\omega$ value for the reagent pair (see above).

Study of the BH_3·LA Catalyzed Reaction of Nitrone 1 with (1-Methoxyvinyloxy)trimethylsilane (5)

Three competitive reactive channels have been characterized for the BH_3·LA-catalyzed reaction between nitrone **1** and silyl ketene acetal **5**. They are related to the two *gauche*, named as *1 gauche* and *2 gauche*, and the *anti* approach modes of the C4–C5 double bond of the silyl ketene acetal **5** to the N2–C3 one of the LA-coordinated nitrone **8** (see Scheme 6). In addition, a TS connecting the [3+2] cycloadduct **9** with *O*-(trimethylsilyl)hydroxylamine (**10**) was also found. Therefore, four TSs (**TS5**, **TS6**, **TS7**, and **TS8**), two intermediates (**IN2** and **IN3**), and the reaction products **9** and **10** were located and characterized. Their total and relative energies are summarized in Table 2, and the geometries of the TSs are given in Figure 3.

TS5 is associated with a concerted 13DC reaction between the LA-coordinated nitrone **8** and silyl ketene acetal **5** to give the [3+2] cycloadduct **9**, while **TS6** and **TS7** correspond to the nucleophilic attack of **5** to **8** in the *2 gauche* and *anti* arrangements to yield the zwitterionic intermediates **IN2** and **IN3**, respectively. A C3–C4 bond rotation at these intermediates converts them into the [3+2] cycloadduct **9** (see Scheme 6). Finally, breaking of the O1–C5 bond and the migration of the TMS group from the O6 oxygen to the nitrone O1 oxygen atom at the cycloadduct **9**, via **TS9**, affords **10**. The activation energies associated with the nucleophilic attack of the silyl ketene acetal **5** to the LA-coordinated nitrone **8** along the three reactive channels are 7.3 (6.8) kcal mol^{-1} for **TS5**, 6.2 (8.2) kcal mol^{-1} for **TS6**,

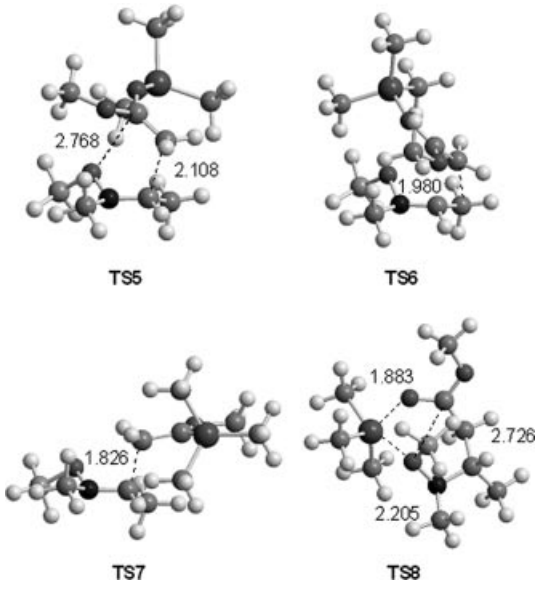

Figure 3. Geometries of the transition structures involved in the addition of the silyloxy enolate **5** to the LA-coordinated nitrone **8** (**TS5**, **TS6**, and **TS7**) and the transition structures involved in the silyl migration (**TS8**). The distances are given in Å.

and 5.4 (13.1) kcal mol^{-1} for **TS7**. For the LA-catalyzed process, the activation energy associated with the concerted [3+2] cycloaddition, **TS5**, is 11.0 kcal mol^{-1} lower in energy than that associated with the uncatalyzed one via **TS2**. In addition, for the LA-catalyzed process the more favorable reactive channel corresponds to the *anti* approach of the silyl ketene acetal **5** to **8**. While formation of the [3+2] cycloadduct **9** is exothermic by –12.5 (–18.1) kcal mol^{-1}, formation of **IN2** is isothermic, 0.0 (3.8) kcal mol^{-1}, and formation of **IN3** is endothermic by 3.7 (13.0) kcal mol^{-1}. The activation energies associated with the conversion of the intermediates **IN3** into **IN2** and **IN2** into **9**, via **TSrot1** and **TSrot2**, are 2.5 (2.0) and 1.3 (0.6) kcal mol^{-1}, respectively. These low values allow the easy conversion of the two intermediates into the thermodynamically more stable cycloadduct **9**.

The activation energy associated with **TS5** is 0.7 kcal mol^{-1} lower in energy than that associated with the more favorable *exo* reactive channel for the IED 13DC between **8** and MVE.[18] This energy result is in agreement with the larger $\Delta\omega$ value for the reaction of **8** + **5** ($\Delta\omega$ = 1.54 eV) than that for the reaction of **8** + MVE ($\Delta\omega$ = 1.40 eV) as a consequence of the more nucleophilic character of silyl ketene acetal **5** than MVE.

The solvent has a contrary effect on the relative energies of the uncatalyzed and catalyzed pathways. Thus, while **TS3** and **IN1** are destabilized by the inclusion of solvent effects, **TS6**, **TS7**, **IN2** and **IN3** are stabilized. This behavior is a consequence of the different solvation of these species with respect to the reagents: while in the uncatalyzed process nitrone **1** has a larger solvation energy than **TS3** and **IN1**, thereby increasing the relative energies, for the catalyzed process the large zwitterionic character of the TSs and intermediates favors the solvation of these species, thereby lowering their relative energies. In addition, solvent produces a change of the relative energies for the catalyzed process. Thus, while in the gas phase the relative stability of the TSs is **TS5** > **TS6** > **TS7**, in the condensed phase the order changes to **TS7** > **TS6** > **TS5**. This behavior can be explained by analyzing the dipole moment of the corresponding TSs: 7.9 D for **TS5**, 10.7 D for **TS6**, and 17.1 D for **TS7**. The gas-phase energy increases with the dipole moment, but with the inclusion of solvent effects the more energetic **TS7** is the most solvated and therefore has the lowest activation energy.

Finally, the activation energy associated with the transformation of the [3+2] cycloadduct **9** into **10** via **TS8** is 14.8 (15.8) kcal mol^{-1}. This barrier is 13.2 kcal mol^{-1} lower in en-

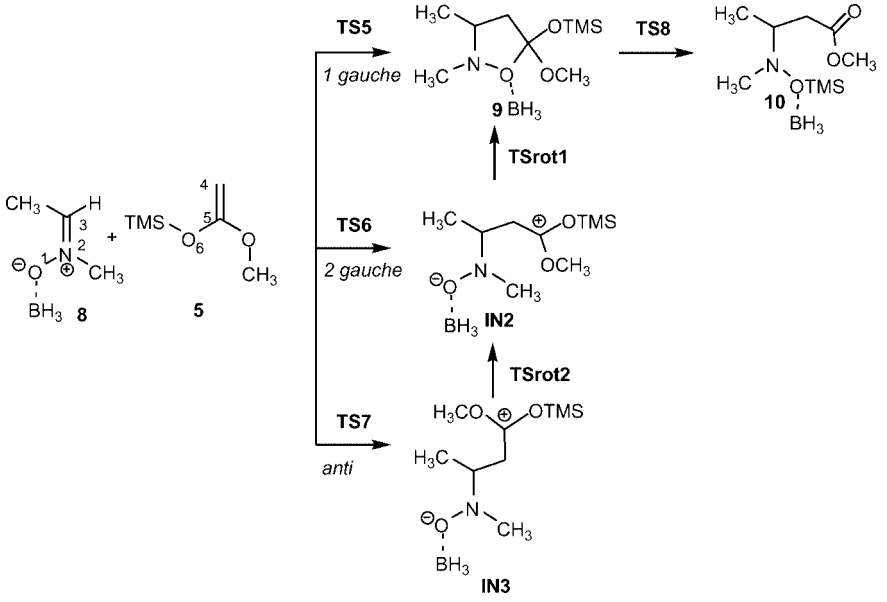

Scheme 6.

ergy than that associated with the conversion of cycloadduct **6** into the hydroxylamine **7** via **TS4**. Consequently, the presence of BH_3·LA coordinated to the O1 atom of the cycloadduct **9** also assists the breaking of the O1–C5 bond and the migration of the TMS group. DFT calculations show that both concerted 13DC and the conversion of **9** into **10** could be competitive, and a mixture of the two products can be obtained experimentally.

The geometries of **TS5**–**TS8** are given in Figure 3. The length of the forming C3–C4 and O1–C5 bonds at the TS associated with the concerted [3+2] cycloaddition (**TS5**) are 2.108 and 2.768 Å, respectively. The asynchronicity at this TS, Δr = 0.66, indicates that it corresponds to a highly asynchronous concerted bond-formation process where only the C3–C4 bond is being formed.[18] This TS is associated with a two-center interaction between the most nucleophilic center of the enolate, the C4 atom, and the most electrophilic center of the nitrone (the C3 atom). The IRC from the *1 gauche* **TS5** to the minimum connects it directly with the [3+2] cycloadduct **9** without the participation of any zwitterionic intermediate. The lengths of the forming C3–C4 bond at the *2 gauche* **TS6** and the *anti* **TS7** are 1.980 and 1.826 Å, while the distances between the O1 and C5 atoms are 3.305 and 4.102 Å, respectively. For the zwitterionic intermediates **IN2** and **IN3** the lengths of the C3–C4 bonds are 1.661 and 1.706 Å, respectively. The N2–C3–C4–C5 dihedral angles at the TSs associated with the attack of enolate **5** to nitrone **8** are –29.2° at the *1 gauche* **TS5**, 39.5° at the *2 gauche* **TS6**, and –169.1° at the *anti* **TS7**.

At the TS associated with the transformation of the [3+2] cycloadduct **9** into **10** (**TS8**), the distances between O1 and C5, O6 and Si, and O1 and Si are 2.726, 2.205, and 1.884 Å, respectively. At this TS, the distance between the O1 and C5 atoms indicates that the O1–C5 bond is already broken.

The BO values of the forming C3–C4 and O1–C5 bonds at the *1 gauche* **TS5** are 0.42 and 0.06, respectively. These values suggest a highly asynchronous concerted TS associated with the attack of the most nucleophilic center of the silyl ketene acetal − the C4 atom − to the most electrophilic center of the nitrone − the C3 atom. Note that the very low O1–C5 BO value at this TS indicates that this bond is not being formed. The BO values of the forming C3–C4 bonds at the *2 gauche* **TS6** and the *anti* **TS7** are 0.52 and 0.63, respectively. Finally, at the intermediates **IN2** and **IN3** the C3–C4 BO values are 0.88 and 0.76, respectively. At **TS8**, the BO values between O1 and C5, O6 and Si, and O1 and Si are 0.00, 0.22, and 0.34, respectively. These BO values indicate that this TS is associated mainly with the TMS migration; the O1–C5 bond is already broken.

To evaluate the CT along the three reactive channels associated with the attack of silyl ketene acetal **5** to LA-coordinated nitrone **8** the natural charges at the TSs were shared between the donor silyl ketene acetal **5** and the acceptor nitrone **8**. The CT from **5** to **8** at the TSs are 0.34 e at **TS5**, 0.33 e at **TS6**, and 0.36 e at **TS7**. These values indicate that these species have some zwitterionic character. For the concerted **TS5** there is a larger CT than that associated with the uncatalyzed process via **TS3**. In addition, the CT at **TS5** is larger than that found at the TS associated with the attack of MVE to **8** (0.24 e)[18] as a consequence of the more nucleophilic character of the silyl ketene acetal **5** than MVE. This large CT allows us to explain the large acceleration of the reaction, which can be associated with the increase of the electrophilicity of the nitrone **1** when coordinated to the boron atom. The CTs at the intermediates **IN2** and **IN3** are 0.72 and 0.52 e, respectively. These large values point out the zwitterionic character of these intermediates.

Conclusions

The molecular mechanisms for the nucleophilic addition of lithium enolates and silyl ketene acetals to nitrones in the absence and in the presence of an LA catalyst to give [3+2] cycloadducts or hydroxylamines have been investigated by DFT methods. Three reaction models have been studied: i) the addition of lithium enolates to nitrones, ii) the addition of silyl ketene acetals to nitrones, and iii) the LA-catalyzed addition of silyl ketene acetals to nitrones. The following conclusions can be drawn from this comprehensive study of these reaction pathways:

i) The addition of lithium enolates to nitrones gives the corresponding adducts, which afford the corresponding hydroxylamines after hydrolysis. Coordination of the lithium atom to the nitrone oxygen atom in an early step of the reaction catalyzes the nucleophilic attack efficiently.

ii) The addition of silyl ketene acetals to nitrones affords the corresponding [3+2] cycloadducts through a concerted 13DC reaction. This cycloaddition reaction has a large activation energy as a consequence of the low electrophilic character of these methyl-substituted nitrones. A further silyl migration on the [3+2] cycloadducts yields the corresponding hydroxylamines.

iii) Finally, the addition of the silyl ketene acetals to LA-coordinated nitrones can take place along three reactive channels associated to two *gauche* and an *anti* approach mode of the C=C double bond of the silyl ketene acetal to the C=N double bond of the nitrone. The *1 gauche* approach mode corresponds to a polar, concerted 13DC reaction to give an isoxazolidinone, while the *2 gauche* and the *anti* approach modes are associated with stepwise nucleophilic attack with formation of the corresponding zwitterionic intermediates. A further bond rotation at these intermediates converts them into the corresponding [3+2] cycloadduct. These three reactive channels are competitive for the LA-catalyzed reactions. A silyl migration on the [3+2] cycloadduct yields the corresponding *O*-silylhydroxylamine. The presence of LA coordinated to the nitrone oxygen atom also catalyzes the migration.

An analysis of the electrophilicity of the reagents accounts for the strong electrophilic character of the LA-coordinated nitrone and the large nucleophilic character of the lithium enolates and silyl ketene acetals. As a consequence of the large electrophilic activation of the nitrone upon coordination of a lithium or boron atom, the mechanism of the reaction changes from a concerted asynchro-

nous cycloaddition with a low polar character and a large activation energy to a concerted highly asynchronous cycloaddition or a stepwise addition with a large polar character and with a low activation energy.

Finally, an analysis of the local indices at the reagents has allowed the characterization of the more electrophilic center of the nitrone − the carbon atom − and the more nucleophilic center of these enolates − the unsubstituted carbon atom. The regioselectivity of these reactions are well explained along the more favorable two-center interaction between the unsubstituted carbon atom of these enolates and the carbon atom of the nitrones.

Computational Methods

DFT calculations were carried out using the B3LYP[25] exchange-correlation functionals, together with the standard 6-31G* basis set.[26] The optimizations were carried out using the Berny analytical gradient optimization method.[27] The stationary points were characterized by frequency calculations in order to verify that the TSs have one, and only one, imaginary frequency. The intrinsic reaction coordinate (IRC)[28] path was traced in order to check the energy profiles connecting each transition structure to the two associated minima of the proposed mechanism by using the second-order González–Schlegel integration method.[29] The electronic structures of stationary points were analyzed by the natural bond orbital (NBO) method.[30] All calculations were carried out with the Gaussian 98 suite of programs.[31] The solvent effects modeled as a continuum model were considered by B3LYP/6-31G* single-point calculations on the gas-phase-optimized geometries using a relatively simple self-consistent reaction field (SCRF)[32] based on the polarizable continuum model (PCM) of Tomasi's group.[33] The electronic energies in solution were obtained by adding the total electrostatic energies obtained from the PCM calculations to the electronic energies in vacuo. The PCM and solvent = dichloromethane options were employed in the SCRF calculations. Recent studies devoted to 1,3-dipolar cycloadditions of nitrones have shown that the inclusion of solvent effects in the total energies give relative energies closer to those obtained using the diffuse function at the 6-31+G* level in vacuo.[18,34] Therefore, we chose to do the energy discussion using the energies in dichloromethane. The global electrophilicity index,[35] ω, which measures the stabilization energy when the system acquires an additional electronic charge, ΔN, from the environment, is given by the simple expression[35] $\omega = (\mu 2/2\eta)$ in terms of the electronic chemical potential, μ, and the chemical hardness, η. Both quantities may be approached in terms of the one-electron energies of the frontier molecular orbitals HOMO and LUMO, ε_H and ε_L, as $\mu \approx (\varepsilon_H + \varepsilon_L)/2$ and $\eta \approx (\varepsilon_L - \varepsilon_H)$, respectively.[36] Beside the global electrophilicity index, it is possible to define its local (or regional) counterpart condensed to atoms.[19] The local electrophilicity index condensed to atom k, ω_k, is easily obtained by projecting the global quantity onto any atomic center k in the molecule by using the electrophilic Fukui function (i.e., the Fukui function for nucleophilic attack, f_k^+).[20] This gives[19] $\omega_k = f_k^+\omega$.

[1] a) A. Cordova, *Acc. Chem. Res.* **2004**, *37*, 102–112; b) M. Arend, B. Westermann, N. Rich, *Angew. Chem. Int. Ed.* **1998**, *37*, 1045–1070; c) E. F. Kleinman, in *Comprehensive Organic Synthesis* (Eds.: B. M. Trost, I. Fleming), Pergamon Press, Oxford, **1991**, vol. 2, p. 893–951.

[2] a) T. Akiyama, A. Suzuki, K. Fuchibe, *Synlett* **2005**, 1024–1026; b) N. Jaber, M. Assie, J.-C. Fiaud, J. Collin, *Tetrahedron* **2004**, *60*, 3075–3084; c) L. D. Bari, S. Guillarme, S. Hermitage, J. A. Howard, D. A. Jay, G. Pescitelli, A. Whiting, D. S. Yufit, *Synlett* **2004**, 708–710; d) M. F. Jacobsen, T. Skrydstrup, *J. Org. Chem.* **2003**, *68*, 7112–7114; e) S. Saaby, K. Nakama, M. A. Lie, R. G. Hazell, K. A. Jorgensen, *Chem. Eur. J.* **2003**, *9*, 6145–6154.

[3] K. Manabe, H. Oyamada, K. Sugita, S. Kobayashi, *J. Org. Chem.* **1999**, *64*, 8054–8057.

[4] a) T. Okino, Y. Hoashi, Y. Takemoto, *Tetrahedron Lett.* **2003**, *44*, 2817–2820; b) C. Qian, L. Wang, *Tetrahedron* **2000**, *56*, 7193–7197; c) T. Kawakami, H. Ohtake, H. Arakawa, T. Okachi, Y. Imada, S.-I. Murahashi, *Bull. Chem. Soc. Jpn.* **2000**, *73*, 2423–2444; d) F. DeGiorgis, M. Lombardo, C. Trombini, *Synthesis* **1987**, 1243–1245.

[5] H.-J. Ha, Y.-G. Ahn, G. S. Lee, *Tetrahedron: Asymmetry* **1999**, *10*, 2327–2336.

[6] a) H.-J. Ha, Y.-G. Ahn, J.-S. Woo, G. S. Lee, W. K. Lee, *Bull. Chem. Soc. Jpn.* **2001**, *74*, 1667–1672; b) T. Mukaiyama, I. Shiina, H. Iwadare, M. Saitoh, T. Nishimura, N. Ohkawa, H. Sakoh, K. Nishimura, Y.-L. Tani, M. Hasegawa, K. Yamada, K. Saitoh, *Chem. Eur. J.* **1999**, *5*, 121–161.

[7] a) S. Jost, Y. Gimbert, A. E. Greene, F. Fotiadu, *J. Org. Chem.* **1997**, *62*, 6672–6677; b) Y. Kita, O. Tamura, F. Itoh, N. Kishino, T. Miki, M. Kohno, Y. Tamura, *Chem. Pharm. Bull.* **1989**, *37*, 2002–2007; c) N. N. Saha, V. N. Desai, D. D. Dhavale, *Tetrahedron* **2001**, *57*, 39–46; d) Y. Tamura, *Chem. Pharm. Bull.* **1989**, *37*, 2002–2007; e) H. Ohtake, Y. Imada, S.-I. Murahashi, *J. Org. Chem.* **1999**, *64*, 3790–3791; f) P. Merino, S. Franco, F. L. Merchán, T. Tejero, *Tetrahedron Lett.* **1998**, *39*, 6411–6414; g) P. Merino, S. Franco, N. Garces, F. L. Merchan, T. Tejero, *Chem. Commun.* **1998**, 493–494.

[8] a) S.-I. Murahashi, Y. Imada, T. Kawakami, K. Harada, Y. Yonemushi, N. Tomita, *J. Am. Chem. Soc.* **2002**, *124*, 2888–2889; b) P. Merino, S. Franco, P. Jimenez, T. Tejero, M. A. Chiacchio, *Lett. Org. Chem.* **2005**, *2*, 302–305.

[9] S. Tomoda, Y. Takeuchi, Y. Nomura, *Chem. Lett.* **1982**, 1787–1788.

[10] T. Kawakami, H. Ohtake, H. Arakawa, T. Okachi, Y. Imada, S.-I. Murahashi, *Chem. Lett.* **1999**, 795–796.

[11] P. Merino, J. A. Mates, *Arkivoc* **2001**, *11*, 12–29.

[12] A. Milet, Y. Gimbert, A. E. Greene, *J. Comput. Chem.* **2005**, *27*, 157–162.

[13] J.-P. G. Seerden, M. M. M. Kuypers, H. W. Scheeren, *Tetrahedron: Asymmetry* **1995**, *6*, 1441–1450.

[14] Indeed, we have also detected the formation of an orthoester in the addition of silyl ketene acetals to chiral nonracemic nitrones. Although only small amounts were obtained, the product could be completely characterized. P. Merino, P. Jimenez, T. Tejero, unpublished results.

[15] L. R. Domingo, M. J. Aurell, P. Pérez, R. Contreras, *Tetrahedron* **2002**, *58*, 4417–4423.

[16] P. Pérez, L. R. Domingo, M. J. Aurell, R. Contreras, *Tetrahedron* **2003**, *59*, 3117–3125.

[17] P. Geerlings, F. De Proft, W. Langenaeker, *Chem. Rev.* **2003**, *103*, 1793–1873.

[18] L. R. Domingo, *Eur. J. Org. Chem.* **2000**, 2265–2272.

[19] L. R. Domingo, M. J. Aurell, P. Pérez, R. Contreras, *J. Phys. Chem. A* **2002**, *106*, 6871–6875.

[20] R. G. Parr, W. Yang, *J. Am. Chem. Soc.* **1984**, *106*, 4049–4050.

[21] M. J. Aurell, L. R. Domingo, P. Perez, R. Contreras, *Tetrahedron* **2004**, *60*, 11503–11509.

[22] K. B. Simonsen, P. Bayón, R. G. Hazell, K. V. Gothelf, K. A. Jorgensen, *J. Am. Chem. Soc.* **1999**, *121*, 3845–3853.

[23] a) L. R. Domingo, S. Gil, R. Mestre, M. T. Picher, *Tetrahedron* **1995**, *51*, 7207–7214; b) G. Asensio, P. Aleman, J. Gil, L. R. Domingo, M. Medio-Simon, *J. Org. Chem.* **1998**, *63*, 9342–9347.

[24] K. B. Wiberg, *Tetrahedron* **1968**, *24*, 1083–1096.

[25] a) A. D. Becke, *J. Chem. Phys.* **1993**, *98*, 5648–5652; b) C. Lee, W. Yang, R. G. Parr, *Phys. Rev. B* **1988**, *37*, 785–789.
[26] W. J. Hehre, L. Radom, P. v. R. Schleyer, J. A. Pople, *Ab initio Molecular Orbital Theory*, Wiley, New York, **1986**.
[27] a) H. B. Schlegel, *J. Comput. Chem.* **1982**, *3*, 214–218; b) H. B. Schlegel, "Geometry Optimization on a Potential Energy Surface", in *Modern Electronic Structure Theory* (Ed.: D. R. Yarkony), World Scientific Publishing, Singapore, **1994**.
[28] K. Fukui, *J. Phys. Chem.* **1970**, *74*, 4161–4163.
[29] a) C. González, H. B. Schlegel, *J. Phys. Chem.* **1990**, *94*, 5523–5527; b) C. González, H. B. Schlegel, *J. Chem. Phys.* **1991**, *95*, 5853–5860.
[30] a) A. E. Reed, R. B. Weinstock, F. Weinhold, *J. Chem. Phys.* **1985**, *83*, 735–746; b) A. E. Reed, L. A. Curtiss, F. Weinhold, *Chem. Rev.* **1988**, *88*, 899–926.
[31] M. J. Frisch, G. W. Trucks, H. B. Schlegel, G. E. Scuseria, M. A. Robb, J. R. Cheeseman, V. G. Zakrzewski, J. Montgomery, J. A., R. E. Stratmann, J. C. Burant, S. Dapprich, J. M. Millam, A. D. Daniels, K. N. Kudin, M. C. Strain, O. Farkas, J. Tomasi, V. Barone, M. Cossi, R. Cammi, B. Mennucci, C. Pomelli, C. Adamo, S. Clifford, J. Ochterski, G. A. Petersson, P. Y. Ayala, Q. Cui, K. Morokuma, D. K. Malick, A. D. Rabuck, K. Raghavachari, J. B. Foresman, J. Cioslowski, J. V. Ortiz, B. B. Stefanov, G. Liu, A. Liashenko, P. Piskorz, I. Komaromi, R. Gomperts, R. L. Martin, D. J. Fox, T. Keith, M. A. Al-Laham, C. Y. Peng, A. Nanayakkara, M. Challacombe, P. M. W. Gill, B. Johnson, W. Chen, M. W. Wong, J. L. Andres, C. Gonzalez, M. Head-Gordon, E. S. Replogle, J. A. Pople, *Gaussian 98*, Revision A.6, Gaussian, Inc., Pittsburgh, PA, **1998**.
[32] a) J. Tomasi, M. Persico, *Chem. Rev.* **1994**, *94*, 2027–2094; b) B. Y. Simkin, I. Sheikhet, *Quantum Chemical and Statistical Theory of Solutions − A Computational Approach*, Ellis Horwood, London, **1995**.
[33] a) E. Cances, B. Mennucci, J. Tomasi, *J. Chem. Phys.* **1997**, *107*, 3032–3041; b) M. Cossi, V. Barone, R. Cammi, J. Tomasi, *Chem. Phys. Lett.* **1996**, *255*, 327–335; c) V. Barone, M. Cossi, J. Tomasi, *J. Comput. Chem.* **1998**, *19*, 404–417.
[34] M. Carda, R. Portoles, J. Murga, S. Uriel, J. A. Marco, L. R. Domingo, R. J. Zaragoza, H. Roper, *J. Org. Chem.* **2000**, *65*, 7000–7009.
[35] R. G. Parr, L. von Szentpaly, S. Liu, *J. Am. Chem. Soc.* **1999**, *121*, 1922–1924.
[36] a) R. G. Parr, R. G. Pearson, *J. Am. Chem. Soc.* **1983**, *105*, 7512–7516; b) R. G. Parr, W. Yang, *Density Functional Theory of Atoms and Molecules*, Oxford University Press, New York, **1989**.

Received: February 7, 2006
Published Online: May 29, 2006

